Delay of Light in an Optical Bottle Resonator with Nanoscale Radius Variation: Dispersionless, Broadband, and Low Loss

M. Sumetsky*

OFS Laboratories, 19 Schoolhouse Road, Somerset, New Jersey 08873, USA

(Received 17 July 2013; published 17 October 2013)

It is shown theoretically that an optical bottle resonator with a nanoscale radius variation can perform a multinanosecond long dispersionless delay of light in a nanometer-order bandwidth with minimal losses. Experimentally, a 3 mm long resonator with a 2.8 nm deep semiparabolic radius variation is fabricated from a 19 μm radius silica fiber with a subangstrom precision. In excellent agreement with theory, the resonator exhibits the impedance-matched 2.58 ns (3 bytes) delay of 100 ps pulses with 0.44 dB/ns intrinsic loss. This is a miniature slow light delay line with the record large delay time, record small transmission loss, dispersion, and effective speed of light.

DOI: 10.1103/PhysRevLett.111.163901 PACS numbers: 42.81.Qb, 42.79.Gn, 42.82.Et

The speed of photons is always equal to the speed of light c. However, a light pulse propagating through an optical structure does not get from point $\mathbf{r}_a$ to point $\mathbf{r}_b$ in time $|\mathbf{r}_a - \mathbf{r}_b|/c$ since it can be absorbed and reemitted, reflected, trapped by a resonant state, travel through a curved waveguide, etc. Regardless of the propagation details the effective speed of light can be determined as $v = L/\tau$, where τ is the actual time of travel from $\mathbf{r}_a$ to $\mathbf{r}_b$ and $L \geq |\mathbf{r}_a - \mathbf{r}_b|$ is the size of the propagation region.

The intriguing problem is to identify the photonic structure with the smallest size L that can perform the required delay τ of a pulse of width $\Delta\tau$ without distortion. The quest for such structures is central in the slow light research [1–6]. Besides general interest, these structures are of great importance for their potential key role as delay lines in optical computing and transformation of data on a chip. For this reason, the research efforts were targeted at the demonstration of a slow light delay line (SLDL) with the smallest dimensions for a given delay time and bandwidth and smallest possible attenuation and dispersion of pulses. Solving this problem is complicated by the fundamental delay-bandwidth product limitation which establishes the smallest possible dimensions of a photonic structure enabling the time delay τ of a pulse with the spectral width $\Delta\lambda$ [7,8].

To arrive at the smallest dimensions, the SLDLs are usually engineered from chains of coupled microresonators with fabrication precision as small as a few nanometers [3]. However, this high precision is still not sufficient for the creation of the smallest possible SLDLs, since nanometer variations in dimensions cause spectral fluctuations comparable with the bandwidth of telecommunication pulses [3–6,9]. In addition, due to material and scattering losses, the attenuation of the miniature SLDL demonstrated to date is very large, measured in the range of 10–100 dB/ns [10], and calls for alternative solutions.

This Letter presents a fundamentally different type of SLDL, which, in contrast to the miniature delay lines considered previously [1–6,10,11], is not based on the photonic structures created by modulation of the refractive index. Instead, the slow propagation of light is ensured by multiple rotations along the surface of a super-low-loss optical fiber—the idea proposed in Ref. [12]. In excellent agreement with the experiment, the theory presented herein shows that a bottle resonator [13–16] formed by nanoscale semiparabolic radius variation of an optical fiber [Fig. 1(a)] can be impedance matched to the input or output waveguide. As a result such a resonator can perform a multinanosecond delay of light at telecommunication

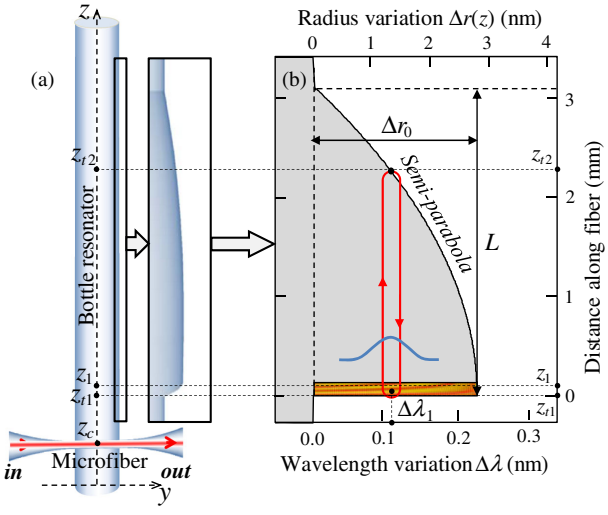

FIG. 1 (color online). (a) Illustration of an optical bottle resonator delay line. Light is coupled into the resonator from a transverse waveguide (microfiber) and experiences whispering gallery mode propagation along the resonator surface. Inset shows the magnified profile of the fiber radius variation. (b) Semiparabolic variation of a bottle resonator radius used in the numerical simulations.

wavelengths within a nanometer-order bandwidth having minimal losses and dispersion.

It is known that the whispering gallery modes (WGMs) propagating along the optical fiber can be fully confined with the dramatically small nanoscale effective radius variation $\Delta r(z) = r(z) - r_0$ [17,18]. In the cylindrical frame of reference (z, ρ, φ), the coordinate dependence of the WGM field is separable and expressed as $\exp(im\varphi)\Lambda_n(\rho)\Psi(z)$, with orbital and radial quantum numbers m and n. For the wavelengths λ close to a resonance cutoff wavelength $\lambda_{\rm res}$ [19], the z dependence of the WGM propagating along the fiber is described by the one-dimensional Schrödinger equation [20]

$$\Psi_{zz} + [E(\lambda) - V(z)]\Psi = 0, \tag{1}$$

with propagation constant $\beta(\lambda, z) = \sqrt{E(\lambda) - V(z)}$. In Eq. (1) the energy $E(\lambda)$ and potential $V(z)$ are determined as

$$E(\lambda) = -\kappa^2 \Delta\lambda/\lambda_{\rm res}, \qquad V(z) = -\kappa^2 \Delta r(z)/r_0, \tag{2}$$

where $\kappa = 2^{3/2}\pi n_r/\lambda_{\rm res}$, $\Delta\lambda = \lambda - \lambda_{\rm res} - i\gamma$, n_r is the refractive index of the fiber, and γ determines the attenuation of light in the fiber. Equation (1) is valid for the adiabatically slow variation of fiber radius $r(z)$, i.e., when $\lambda_{\rm res}^2 r_0^{-1} dr(z)/dz \ll \Delta\lambda_{\rm res}$, where $\Delta\lambda_{\rm res}$ is the separation of $\lambda_{\rm res}$ from the adjacent cutoff resonance [19]. This condition is well satisfied for the smooth nanoscale variation $\Delta r(z)$ considered below.

Light in the bottle resonator is confined between turning points z_{t1} and z_{t2} [determined as zeros of the propagation constant, $\beta(\lambda, z_{tj}) = 0$] and coupled to the input or output microfiber waveguide at contact point z_c as illustrated in Fig. 1(a). Since the microfiber diameter (usually ~ 1 μm) is much smaller than the characteristic axial wavelength of $\Psi(z)$ (≥ 10 μm), coupling to the microfiber can be approximated in Eq. (1) by adding the δ-function potential $D\delta(z - z_c)$ and source $C\delta(z - z_c)$ with complex-valued coupling parameters C and D. In this approximation the transmission amplitude $S(\lambda, z_c)$ through the microfiber coupled to the bottle resonator and the corresponding group delay of light $\tau(\lambda, z_c)$ are [20]

$$\begin{aligned} S(\lambda, z_c) &= S_0 - \frac{i|C|^2 G(\lambda, z_c, z_c)}{1 + DG(\lambda, z_c, z_c)}, \\ \tau(\lambda, z_c) &= \frac{\lambda^2}{2\pi c}\,\mathrm{Im}\left(\frac{\partial \ln S(\lambda, z_c)}{\partial\lambda}\right), \end{aligned} \tag{3}$$

where S_0 is the out-of-resonance amplitude and $G(\lambda, z_1, z_2)$ is the Green's function of the uncoupled bottle resonator defined by Eq. (1) with boundary conditions $\Psi(z) \to 0$ at large positive $z - z_{t2}$ and $z_{t1} - z$. For elongated bottles with slow and smooth radius variation, the solution of Eq. (1) can be found in the semiclassical approximation [21] (for details see Supplemental Material [22]),

$$\begin{aligned} G(\lambda, z, z) &= \frac{\cos[\varphi(\lambda, z_{t1}, z) + \chi_1]\cos[\varphi(\lambda, z, z_{t2}) + \chi_2]}{\beta(\lambda, z_1)\sin[\varphi(\lambda, z_{t1}, z_{t2}) + \chi_1 + \chi_2]}, \\ \varphi(\lambda, z_1, z) &= \int_{z_1}^{z} \beta(\lambda, z) dz. \end{aligned} \tag{4}$$

where parameters $\chi_j \sim 1$ are the phase increments near the turning points z_{tj}.

A light pulse launched from the input microfiber into the bottle resonator at contact point z_c slowly propagates along the resonator axis in both directions and returns back after reflecting from turning points z_{t1} and z_{t2}. Generally, after completing the round-trip between one of the turning points and the contact point, the pulse does not fully return back into the microfiber output and is partly reflected into the resonator. The reflection at z_c determines the impedance mismatch between the input and output microfiber and resonator and causes bouncing of the pulse between turning points with decreasing amplitude. In the stationary formulation described by Eqs. (3) and (4), oscillations of the pulse correspond to oscillations of the transmission amplitude and group delay as a function of wavelength. Averaging the group delay found from Eqs. (2)–(4) over the local period of these oscillations yields the average group delay, which, for relatively small coupling loss [11], coincides with the classical time of the round-trip propagation along the bottle resonator

$$\overline{\tau(\lambda)} = \frac{\lambda_{\rm res}^2}{\pi c}\int_{z_{t1}}^{z_{t2}} \frac{\partial\beta(\lambda, z)}{\partial\lambda} dz. \tag{5}$$

From Eq. (4) the smallest period of oscillations coincides with the local spacing between the axial eigenvalues of the uncoupled bottle resonator equal to $\Delta\lambda_S = \lambda_{\rm res}^2/c\overline{\tau(\lambda)}$. Suppression of these oscillations leads to the condition of impedance matching when the pulse is fully transmitted from the microfiber input into the bottle resonator and, after completing the round-trip along the resonator axis z, it is fully transmitted back into the microfiber output.

Remarkably, it is possible to solve the impedance matching problem for the bottle resonator locally near wavelength λ_i without modification of the bottle profile $\Delta r(z)$ [23]. As shown in the Supplemental Material [22], the oscillations of transmission amplitude and group delay are suppressed at wavelength λ_i at a microfiber position z_i which is close to turning point z_{t1} if

$$\mathrm{Im}(S_0) = 0, \qquad |C|^2 = 2S_0\,\mathrm{Im}(D), \tag{6}$$

$$\begin{aligned} \beta(\lambda_i, z_i) &= \mathrm{Im}(D), \\ \mathrm{Im}(D)/\mathrm{Re}(D) &= \tan[\varphi(\lambda_i, z_{t1}, z_i) + \chi_1]. \end{aligned} \tag{7}$$

Equation (6) is the condition of lossless coupling between the microfiber and resonator [20] when the considered SLDL is all-pass and, hence, has no transmission power oscillations. Equation (7) establishes the additional relations between λ_i, z_i, and coupling parameter D which

allow the group delay oscillations to vanish as well. These impedance matching conditions are illustrated in the numerical example below and also approximately achieved in the experimentally demonstrated SLDL.

To avoid dispersion, the eigenfrequencies of the bottle resonator should be locally equidistant, which is typical for large and smooth quantum wells $V(z)$ away from their bottom. However, the slowest axial speed of light corresponds to the bottom of quantum well. To arrive at the dispersionless propagation with the smallest possible speed, the shape of the bottle resonator in this region should have the equidistance frequency spectrum. This condition is satisfied for the bottle resonator with semiparabolic radius variation $\Delta r(z) = \Delta r_0 - z^2/(2R)$ for $0 < z < L = (2R\Delta r_0)^{1/2}$ and $\Delta r(z) = 0$ elsewhere [Fig. 1(b)]. Here R is the axial curvature of the bottle resonator and L is its length. The classical wavelength-independent time delay in this structure found from Eq. (5) is

$$\tau = 2^{-1/2}\pi n_r L(r_0/\Delta r_0)^{1/2}/c. \tag{8}$$

The parameters of a semiparabolic bottle SLDL in Fig. 1 are chosen to model the experiment below (resonator length $L = 3$ mm, fiber radius $r_0 = 19$ μm, semiparabola height $\Delta r_0 = 2.8$ nm, fiber refractive index $n_r = 1.46$, and material attenuation $\gamma = 0.1$ pm). For these parameters, Eq. (8) yields the delay time $\tau = 2.67$ ns and effective speed of light $L/\tau = c/267$. Figures 2(a) and 2(b) are the surface plots of the resonance amplitude and group delay distributions as a function of wavelength and distance along the bottle resonator in the vicinity of z_{t1}, where the impedance matching conditions [Eqs. (6) and (7)] are satisfied at wavelength variation $\Delta\lambda_1$ and coordinate z_1. The spectral profiles crossing the impedance matched point $(\Delta\lambda_1, z_1)$are shown in Figs. 2(c) and 2(d). The amplitude and group delay ripples vanish at $(\Delta\lambda_1, z_1)$ and are relatively small in the neighborhood of this point. Figure 2(e) shows the time domain propagation of a 100 ps pulse through the constructed SLDL [the amplitude spectrum of the pulse is depicted in Fig. 2(c)]. It is seen that the spurious temporal ripples at the output are remarkably small ($<8.5\%$ in magnitude [Fig. 3(b)] and thus $<0.7\%$ in intensity) and the FWHM pulse broadening in Fig. 3(b) is negligible. The average delay time found from the spectrum in Fig. 2(d) and from the time domain calculation in Fig. 2(e) is in excellent agreement with the value 2.67 ns found from Eq. (8).

An SLDL enabling the dispersionless delay of a pulse with a different temporal width $\Delta\tau_s = s\Delta\tau$ and the same delay time τ can be simply constructed by rescaling the height of the parabola Δr_0 and its length L to

$$\Delta r_s = s^{-1}\Delta r_0, \qquad L_s = s^{-1/2}L. \tag{9}$$

The magnitude of spurious ripples of the new delay line remains the same (see Supplemental Material [22]).

Experimentally, the 3 mm long bottle resonator SLDL was created at the 19 μm radius optical fiber with the

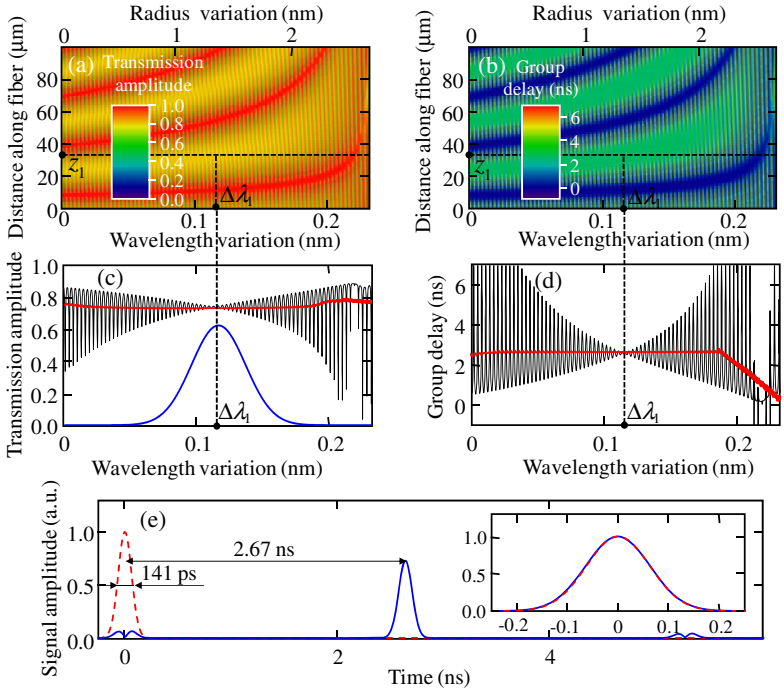

FIG. 2 (color online). (a),(b) Surface plots of the transmission amplitude and group delay near the edge $z = z_{t1}$ of the bottle resonator calculated with the coupling parameters defined in the text. (c),(d) Transmission amplitude and group delay spectra at the coupling point $z_c = z_1$ shown in (a) and (b), respectively. (e) The output signal amplitude (solid line) calculated for the input 100 ps pulse (dashed line). The pulse spectrum is determined by the bold line in (c).

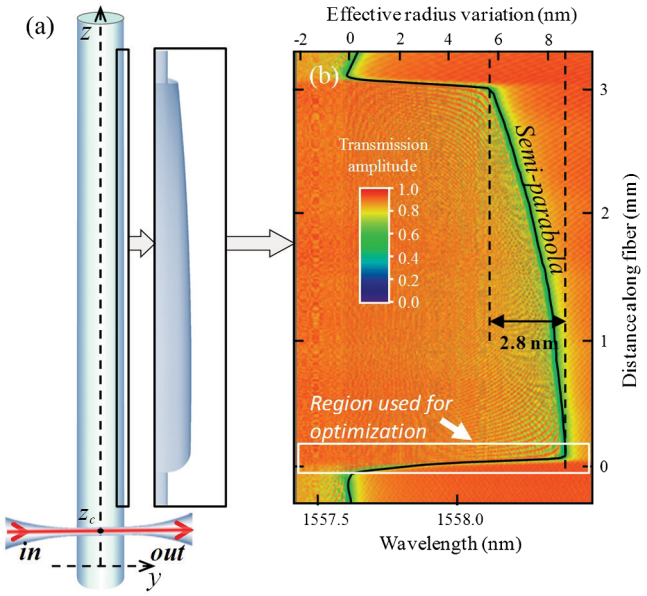

FIG. 3 (color online). (a) Illustration of an optical bottle resonator delay line. Inset shows the magnified profile of the fiber radius variation. (b) Experimentally measured surface plot of the transmission amplitude measured at microfiber positions spaced by 10 μm along the fiber axis, which was used to determine the bottle resonator radius variation (bold line).

surface nanoscale axial photonics (SNAP) technology, which enables the predetermined nanoscale modification of the optical fiber radius with the record subangstrom precision by annealing with a focused CO_2 laser beam [20,24]. The speed of the beam was varied to ensure the required nanoscale semiparabolic profile of $\Delta r(z)$. The introduced radius variation $\Delta r(z)$ was calculated using Eqs. (2)–(4) from the surface plot of resonance spectra, which was measured at microfiber positions spaced by 10 μm along the fiber axis [20,25,26] [Fig. 3(b)]. The depth of $\Delta r(z)$ is 8 nm, while the parabolic part of $\Delta r(z)$ has the depth of 2.8 nm and was introduced with a precision of better than 0.9 Å.

The values of coupling parameters C and D were optimized by translation of the microfiber taper with respect to the bottle resonator to arrive at two sets of wavelengths and contact points with suppressed oscillations of the group delay and transmission amplitude. These sets, (λ_1, z_1), and (λ_2, z_2) [Figs. 4(a) and 4(b)] correspond to the same y coordinate of the microfiber taper and, hence, to the same microfiber-to-resonator coupling parameters C and D. At contact point z_1, the vicinity of wavelength λ_1 [Figs. 4(a)–4(d)] corresponds to the propagation of light near the top of quantum well $V(z)$. This case is used below as a reference. At contact point z_2, the vicinity of wavelength λ_2 [Figs. 4(a), 4(b), 4(e), and 4(f)] correspond to the slowest propagation in the parabolic part of quantum well $V(z)$, the case of our main interest.

Figures 4(g) and 4(h) show the time-dependent propagation of a 100 ps Gaussian pulse calculated from the

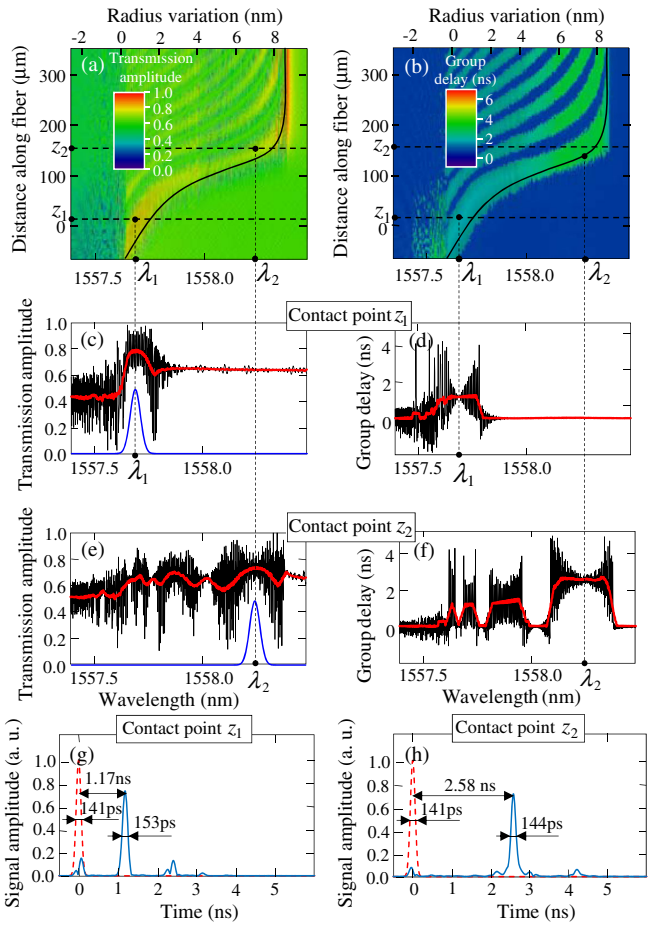

FIG. 4 (color online). (a),(b) Surface plots of the transmission amplitude and group delay near the edge $z = z_{t1}$ of the fabricated bottle resonator measured after the optimization of coupling parameters by translation of the microfiber with respect to the resonator. (c),(d) Transmission amplitude and group delay spectra at the coupling point $z_c = z_1$ corresponding to minimum spectral oscillations in (a) and (b), respectively. (e),(f) The same as (c),(d) but at the coupling point $z_c = z_2$, which corresponds to the semiparabolic part of the potential $V(z)$. (g),(h) The output signal amplitudes (solid line) calculated for the input 100 ps pulse (dashed line) from the spectra measured at points z_1 and z_2, with the pulse spectrum determined by the bold line in (c) and (e), respectively.

measured spectra shown in Figs. 4(c)–4(f), respectively. The average group delays in Figs. 4(d) and 4(f) are in excellent agreement with the delay times 1.17 and 2.58 ns in Figs. 4(g) and 4(h). Comparison of the average transmission amplitudes in Figs. 4(c) and 4(e) and the corresponding delay times determines the intrinsic loss of the demonstrated device equal to 0.44 dB/ns.

Since the optimization was performed only approximately, out-of-resonance coupling losses ~2 dB (irrelevant to intrinsic losses and, thus, independent of the delay time) were introduced. However, even in this case, the total insertion loss of the 2.58 ns (3 bytes) delay line has the impressive record value of 3 dB, i.e., 1.12 dB/ns, as

compared to 10–100 dB/ns losses previously demonstrated for miniature delay lines [3–6,10]. The spurious temporal ripples in Fig. 4(h) are remarkably small ($<11\%$ in magnitude and thus $<1.2\%$ in intensity) and the FWHM pulse broadening is negligible [$<3\%$, which is 4 times smaller than the pulse broadening for significantly smaller delay in Fig. 4(g)]. In addition, the effective speed of light in this SLDL is $c/258$, the record small for the engineered slow light photonic structures [3–6].

In summary, the demonstrated bottle resonator with nanoscale radius variation is a fundamentally different type of a slow light delay line not based on periodic modulation of the refractive index. It presents a solution to the central problem of the slow light research—creation of a miniature delay line with a breakthrough performance. This demonstration also emphasizes the flexibility of the SNAP platform [20,24] as a fruitful source for exciting fundamental and applied studies. A similar approach will allow creating a variety of photonic structures that precisely imitate one-dimensional quantum mechanical structures described by the potential $V(z)$ under interest. This includes potential structures that can be used for investigation of tunneling and time delay [27–29], Anderson localization [30,31], localized states in continuum [32,33], etc. This also includes intriguing opportunities for creating photonic microdevices for filtering, switching, lasing, delay of light, and sensing with unprecedented high precision and low loss.

The author is grateful to Y. Dulashko for assisting in the experiments and to D. J. DiGiovanni, T. Kremp, and V. Mikhailov for helpful discussions.

*Present address: Aston Institute of Photonic Technologies, Aston University, Birmingham B4 7ET, England.

[1] A. Yariv, Y. Xu, R. K. Lee, and A. Scherer, Opt. Lett. **24**, 711 (1999).
[2] M. F. Yanik and S. Fan, Phys. Rev. Lett. **92**, 083901 (2004).
[3] F. N. Xia, L. Sekaric, and Y. Vlasov, Nat. Photonics **1**, 65 (2007).
[4] M. Notomi, E. Kuramochi, and T. Tanabe, Nat. Photonics **2**, 741 (2008).
[5] M. Notomi, Rep. Prog. Phys. **73**, 096501 (2010).
[6] F. Morichetti, C. Ferrari, A. Canciamilla, and A. Melloni, Laser Photonics Rev. **6**, 74 (2012).
[7] G. Lenz, B. J. Eggleton, C. K. Madsen, and R. E. Slusher, IEEE J. Quantum Electron. **37**, 525 (2001).
[8] D. A. B. Miller, Phys. Rev. Lett. **99**, 203903 (2007).
[9] M. L. Cooper, G. Gupta, M. A. Schneider, W. M. J. Green, S. Assefa, F. Xia, Y. A. Vlasov, and S. Mookherjea, Opt. Express **18**, 26 505 (2010).
[10] S. A. Schulz, L. O'Faolain, D. M. Beggs, T. P. White, A. Melloni, and T. F. Krauss, J. Opt. **12**, 104004 (2010).
[11] M. Sumetsky, Opt. Express **21**, 15 268 (2013). In this paper, a miniature SNAP delay line based on 20 coupled microresonators was demonstrated. However, this delay line was strongly dispersive and the impedance match to the input-output waveguide had not been achieved.
[12] A. B. Matsko, A. A. Savchenkov, and L. Maleki, in *Optical Amplifiers and Their Applications/Coherent Optical Technologies and Applications, Technical Digest (CD)* (Optical Society of America, Washington, DC, 2006), paper CThD5.
[13] M. Sumetsky, Opt. Lett. **29**, 8 (2004).
[14] Y. Louyer, D. Meschede, and A. Rauschenbeutel, Phys. Rev. A **72**, 1 (2005).
[15] G. S. Murugan, J. S. Wilkinson, and M. N. Zervas, Opt. Express **17**, 11916 (2009).
[16] M. Pöllinger, D. O'Shea, F. Warken, and A. Rauschenbeutel, Phys. Rev. Lett. **103**, 053901 (2009).
[17] M. Sumetsky and J. M. Fini, Opt. Express **19**, 26470 (2011).
[18] The effective radius variation includes the variation of the physical radius as well as of the refractive index. In addition, it is calculated by averaging the actual radius and index variations over the cross section of the fiber.
[19] A. W. Snyder and J. D. Love, *Optical Waveguide Theory* (Chapman and Hall, London, 1991).
[20] M. Sumetsky, Opt. Express **20**, 22 537 (2012).
[21] L. D. Landau and E. M. Lifshitz, *Quantum Mechanics* (Pergamon, New York, 1965), 2nd ed.
[22] See Supplemental Material at http://link.aps.org/supplemental/10.1103/PhysRevLett.111.163901 for details.
[23] The impedance matching problem has been addressed previously for the coupled resonator and photonic crystal delay lines by "apodization" of parameters of these structures in the vicinity of the input and output waveguide (see, e.g., Refs. [4–6]). Analogously, more accurate impedance matching between the bottle resonator and the microfiber can be achieved by modification of fiber radius variation in the vicinity of contact point z_c.
[24] M. Sumetsky and Y. Dulashko, Opt. Express **20**, 27 896 (2012).
[25] T. A. Birks, J. C. Knight, and T. E. Dimmick, IEEE Photonics Technol. Lett. **12**, 182 (2000).
[26] M. Sumetsky and Y. Dulashko, Opt. Lett. **35**, 4006 (2010).
[27] H. Winful, Phys. Rep. **436**, 1 (2006).
[28] M. Tomes, K. J. Vahala, and T. Carmon, Opt. Express **17**, 19 160 (2009).
[29] C. A. A. de Carvalho and H. M. Nussenzveig, Phys. Rep. **364**, 83 (2002).
[30] Y. Lahini, R. Pugatch, F. Pozzi, M. Sorel, R. Morandotti, N. Davidson, and Y. Silberberg, Phys. Rev. Lett. **103**, 013901 (2009).
[31] M. Segev, Y. Silberberg, and D. N. Christodoulides, Nat. Photonics **7**, 197 (2013).
[32] F. Capasso, C. Sirtori, J. Faist, D. L. Sivco, S. N. G. Chu, and A. Y. Cho, Nature (London) **358**, 565 (1992).
[33] Y. Plotnik, O. Peleg, F. Dreisow, M. Heinrich, S. Nolte, A. Szameit, and M. Segev, Phys. Rev. Lett. **107**, 183901 (2011).